Environmental Resources Research
Vol. 8, No. 1, 2020

GUASNR

Study of kinetics, isotherms and thermodynamics of lead adsorption from aqueous solutions using Lignocellulose Nano-fibers (LCNFs)

S. Rastgar[1], H. Rezaei[2*], H. Yousefi[3]

[1]Ph.D candidate, Gorgan University of Agricultural Sciences and Natural Resources, Gorgan, Iran
[2]Assistant Professor, Department of Environmental Pollution, Gorgan University of Agricultural Sciences and Natural Resources, Gorgan, Iran
[3]Associate Professor, Department of Wood and Paper Engineering, Gorgan University of Agricultural Sciences and Natural Resources, Gorgan, Iran

Received: January 2019 ; Accepted: December 2019

Abstract

The surface adsorption of heavy metals in effluents with nanoparticles is today a suitable method for effluents treatment. In the present study, lignocellulose nano-fibers (LCNFs) were used as natural adsorbent for lead adsorption. The aim was to evaluate lead adsorption using adsorption isotherms, kinetics and thermodynamics. Fourier Transform-Infrared Spectroscopy (FT-IR) and Transmission Electron Microscopy (TEM) were employed to determine the chemical and structural properties of this adsorbent. To study the adsorption isotherm, two-parameter models of Langmuir, Freundlich, Temkin, and Dubinin–Radushkevich were compared and three-parameter models of Redlich-Peterson and Sips and maximum correlation coefficient (R^2) were selected as the best isotherm model for lead adsorption, which was obtained for the Langmuir model at 0.9997 and the Redlich-Peterson model at 0.9338. Therefore, the data were consistent with both models but were better described by the Langmuir model, indicating homogeneity of the adsorbent surface. In addition, reaction kinetic models, including pseudo-zero-order, pseudo-first-order, pseudo-second-order and pseudo-third-order as well as the diffusion kinetic models including intra-particle diffusion and Elovich were investigated for adsorption reaction. The maximum correlation coefficient (R^2=1) was related to the pseudo-second-order model; therefore, the lead adsorption by LCNFs was of a chemical type. The results obtained from the calculation of thermodynamic parameters such as Gibbs free energy (ΔG), enthalpy (ΔH◦), and entropy (ΔS◦) respectively showed spontaneity, exothermicity, and increased irregularities of the reaction. This study showed that LCNF is suitable for the adsorption of lead and as such could be used as a cost-effective adsorbent in the process of industrial wastewater treatment.

Keywords: Adsorption, isotherm, kinetics, lignocellulose Nano-fibers (LCNFs), lead.

[*]Corresponding author; hassanrezaei@gau.ac.ir

Introduction

Industrial development in recent years has led to an increase in the volume of sewage and wastewater. The defective and non-standard disposal of these wastewaters causes the release of large amounts of heavy metals into aquatic ecosystems (Kini Srinivas et al., 2013). Heavy metals have bio-accumulative property whose toxic effects on living organisms are chronic (Betancur et al., 2009). The most common metals found in sewage include lead, copper, cadmium, chromium and nickel. Among these, lead is the most widespread heavy element and toxic, which happens due to the discharge of large quantities of industrial wastewater in contact with or including batteries, paint, glass, printing, etc. (Yu et al., 2001). Some of the effects of lead on humans are damages to the kidneys, liver, brain and heart as well as anemia, and seizures. Accordingly, it is essential to remove or reduce lead from sewage and industrial effluents (Ozcan et al., 2007). According to researches, adsorption is the most appropriate and most widely used technique for heavy metal removal. The most important benefits of the adsorption system are less investment, simple design and easy operation, less energy consumption and high removal efficiency of contaminants compared to chemical, physical and biological treatment processes (Melichova and Romada, 2013; Reddy and Lee, 2013). To comprehensively study the adsorption reaction of heavy metals in water, familiarity with the concepts of equilibrium isotherm, kinetics and thermodynamics of adsorption is essential, and such studies are complementary. The adsorption isotherms with the help of equilibrium data and absorption properties describe how adsorbents react with pollutants and play an essential role in optimizing adsorbent consumption (Shahat et al., 2015).

The kinetics of the adsorption process should be studied to control the steps of the reaction rate and to evaluate the factors affecting the reaction rate. Thermodynamics is a branch of natural science dealing with heat and its relation to energy and work (Elagiwu et al., 2009). Various researchers worked on modeling of kinetics, isotherms and thermodynamics of adsorption by lignocellulose and its derivatives (lignin and cellulose) on nano- and micro-scales. Some cases are mentioned below.

Yang et al. (2014) used cellulose nanofiber composite and alcohol to remove chromium and lead, and examined Langmuir and Freundlich isotherms. Their results indicated that the data were compatible with both isotherms.

Kardam et al. (2014) exploited cellulose nanofiber as an adsorbent to remove cadmium, nickel and lead from aqueous solutions, as well as Langmuir and Freundlich equilibrium isotherms; the data for each of the three metals followed both models.

Lopicic et al. (2016) removed copper with lignocellulose. Their results on isotherms, kinetics and thermodynamics of adsorption showed that the data were more consistent with Elovich isotherm and the second-order kinetics, as well as the reactions were exothermic.

Largitte et al. (2016) used lignocelluloses to remove lead, and investigated kinetics and thermodynamics and isotherms of adsorption. Data were matched with Elovich kinetics, Langmuir and Freundlich isotherms, and the reaction was endothermic.

Bhutto et al. (2016) remove the lead with activated carbon from lignocellulose. They studied kinetics, thermodynamics and isotherms of adsorption. The data were more consistent with Freundlich isotherm and intra-particle diffusion kinetics. The results of thermodynamic studies showed that the experiment was of endothermic and spontaneous type.

Samana et al. (2017) used lignocellulose wastes to remove mercury, and evaluated adsorption kinetics and isotherms. The data were more consistent with the intra-particle diffusion, as well as the Temkin and Langmuir isotherms.

The purpose of this study was to study three important issues of isotherms, kinetics and thermodynamics in order to understand completely the lead adsorption by LCNFs. The two-parameter models (Langmuir,

Freundlich, Dubinin-Radushkevich and Temkin) and three-parameter models (Sips and Redlich-Peterson) were used to test the adsorption isotherm. Investigating the kinetics of lead adsorption using reaction kinetic models (pseudo-zero-order, pseudo-first-order, pseudo-second-order and pseudo-third-order), and diffusion kinetic models (intraparticle diffusion and Elovich) as well as the lead adsorption thermodynamics were investigated using a temperature variation study. The present study was undertaken to test the biosorption efficiency of this LCNF for lead from the aqueous solutions. For each topic, the data from the models were compared with the empirical data to detect the best model.

Materials and Methods

Materials

The LCNFs gel was purchased from Nano Novin Polimer Co. (Sari, Iran). It should be noted that lignocellulosic pulp (including lignin and hemicellulose) was made from beech, common hornbeam and cottonwood trees. Pb $(NO_3)_2$. $6H_2O$, HCL and NaOH to adjust pH were Merck (Germany). Double-distilled water was used for batch experiments and dilution. The pH was adjusted using 0.1 M NaOH and 0.1 M HCl. The stock solution (1000 mg/L) was prepared from Pb $(NO_3)_2$ in deionized water. Other metal solutions required for further experiments were prepared from this solution. The standard lead stock (1000 mg/L) was prepared with deionized water and Pb $(NO_3)_2.6H_2O$; thus, 1000 mg (1 g) of lead was dissolved in 1 liter of deionized water. Based on the molecular mass of lead nitrate (331.02g/mol), the molecular weight of lead (207.02g/mol) and the purity of lead nitrate (99%), the amount (gram) of lead salt required to make this solution was calculated to be about 1.598 g. The nitrate salt was diluted with the deionized water in a 1000-liter volumetric flask. Other test solutions were prepared daily by diluting the stock solution with the deionized water.

Analysis and identification equipment

The devices used for testing included Atomic Absorption Spectroscopy (AAS, Unicam-919) to obtain the final equilibrium concentration (absorbed heavy metal concentration), pH meter (AZ86552) to measure pH, incubator shaker (IKA KS 4000 ic, Germany) for mixing adsorbent and adsorbate according to the parameters tested, Centrifuge (HERMLE Z300, the USA) for separating suspended particles from the solution, digital scale (BANDS, BS-3003) to weight adsorbent and lead with high accuracy. The FT-IR apparatus (WQF-520) was used to characterize the molecules and functional groups. The TEM device (Zeiss-EM10C) was applied to determine the size distribution of LCNFs and its characteristics.

Lead adsorption tests

Lead adsorption test was performed using adsorbent LCNFs in a batch sytem and pilot scale. To investigate the effects of pH, time, temperature, adsorbent dosage, initial concentrations of 100 milliliter lead metal in a 250 milliliter elastomer, a certain amount of adsorbent was added to each flask and placed on the shaker. After completion of the reaction time, the adsorbent was separated from the solution by centrifuge at 4000 rpm for 5 minutes. Then the liquid supernatant was discarded and used to determine the amount of absorbed metal by the atomic absorption device. All adsorption experiments were conducted in a batch system. The effect of each parameter in all stages of the experiment was studied by changing the desired and constant parameters considering other parameters mentioned.

Conditions and factors affecting the adsorption process were initial lead concentration (10-50 mg/L), pH (4-8), adsorbent dosage (0.1-1 g), temperature (15-40 °C), and contact time (15-120 min). In order to better compare the effects of the factors studied, the other parameters were kept constant under optimal conditions of pH=6, 25 °C, contact time of 60 min, initial lead concentration of 10 mg/L and adsorbent dosage of 0.3 g. At the end of each experiment, the percentage of lead

removal and adsorption dosage (mg/g) was calculated using the following equations. The removal percentage and adsorption capacity of lead metal in equilibrium status by LCNFs were calculated, respectively, through equations 1 and 2 (Inagaki et al., 2013 and Niknahad Gharmakher et. al., 2018).

$$\%\text{Removal} = \frac{(C_o - C_e)}{C_o} \times 100 \quad (1)$$

$$q = \frac{(C_o - C_e)v}{M} \quad (2)$$

Where, qe is the amount adsorbed per unit mass of adsorben in mg/g, C_o: initial metal concentration before adsorption in $mg.l^{-1}$, C_e: the remaining metal concentration in solution at equilibrium after adsorption in mg/g, V: the solution volume in lit, and M: the adsorbent mass in g (Salamat et al. 2019). It should be noted that all experiments were repeated three times, and the mean data and results were used.

Assessment method of adsorption isotherms (equilibrium model)

The initial lead concentration (10 mg/L) was prepared to evaluate the adsorption isotherm. The pH of the solutions was adjusted to be 6. Different adsorbent dosages (0.1, 0.3, 0.6, 0.8 and 1 g) of LCNFs were added to each solution and then stirred at a temperature of 25 °C inside the incubator shaker for 60 min. Finally, the used flasks were taken from the incubator shaker (at 4000 rpm and 5 min) and then the centrifuge made a two-phase solution. The remaining heavy metal solution was measured by atomic absorption spectroscopy. The data from the equilibrium isotherm were achieved from the data of this section. Then, empirical data matching with equilibrium models (two-parameter models of Langmuir, Freundlich, Temkin and Dubinin-Radushkevich and three-parameter models of Redlich-Peterson and Sips) was investigated, and the curves for each model were drawn using its linear and nonlinear forms presented in Table 1. In the Langmuir isotherm model, it is assumed that the adsorbate interacts only with a limited number of uniform adsorption sites and adsorption is limited to a single monolayer on the surface (Huang et al., 2015). The fundamental feature of the Langmuir isotherm is shown using a constant without a unit called the equilibrium parameter R_L whose equation is given below.

$$R_L = \frac{1}{1 + bC_e} \quad (3)$$

$R_L > 1$ represents undesirable isotherm, $R_L = 1$ means linear isotherm, $0 < R_L < 1$ is desirable isotherm and $R_L = 0$ shows irreversible isotherm (Parhizgar et. al., 2017).

Freundlich model is based on the multilayer adsorption on uneven surface and heterogeneous energy distribution on the adsorbent active sites (Wang et al., 2010). The Doubinin-Radushevich model is often used to determine the nature and characteristics of the adsorption process and to measure free energy. If the free energy (E in $Kj.Mol^{-1}$) obtained from this model is less than 8, the adsorption will be in physical type due to the weak Van der Waals forces and if it is in the range of 8 to 16, the metal ion will be adsorbed by the ion exchange mechanism.

When E is between 20 and 40, adsorption will be of chemical type (Kolodynska et al., 2017; Afzal Kamboh et al., 2016). In the Temkin adsorption isotherm model, positive or negative values of B_T indicate an exothermic or endothermic process of adsorption (Alam Khan et al., 2016). Of the three-parameter isotherm models, the Redlich-Peterson model often refers to the adsorption of the liquid phase of heavy metals and organic compounds (Arvind et al., 2017). The Sips isotherm combines the Freundlich and Langmuir isotherm, and predicts heterogeneous adsorption processes (Nethaji et al., 2013).

Table 1. Constant coefficients of isotherm models used in this research.

Constant coefficients	Linear form	Main equation	Isotherm type	References
K_f: Freundlich constant, indicating adsorption capacity (mg/g) $(L.g^{-1})^{1/n}$ n: Freundlich constant, indicating adsorption intensity	$Logq_e = logk_f + \frac{1}{n} LogC_e$	$q = k_f C_e^{1/n}$	Freundlich	Sekar et al. (2004),Nagpal et. al. (2010)
C_e: Final adsorbate concentration in solution after equilibrium (mg/L) q_e: adsorbate amount in equilibrium conditions (mg/g) q_m: Adsorption capacity (mg/g) b: Langmuir constant $(L.mg^{-1})$	$\frac{C_e}{q_e} = \frac{1}{q_m b} + \frac{C_e}{q_m}$	$q_e = \frac{q_m \times C_e b}{1 + C_e b}$	Langmuir	Shahmohaammadi Kalagh et al. (2011)
B_T: Temkin isotherm constant $(kJ.mol^{-1})$ A_T: Binding constant, indicating maximum binding energy $(L.g^{-1})$	$q_{e=} \frac{RT}{b} Ln(A_T C_e)$	$q_e = B_T LnA_T + B_T LnC_e$	Temkin	Ahmad et al. (2005); Mohammad (2013)
ε: Polanyi potential adsorption $(KJ^2.mol^{-2})$ B: Moderate free energy of adsorption $(mol^2.kj^{-2})$ R: Gases constant $(J.mol^{-1}.k^{-1})$ T: Temperature (k)	$q_{e=}exp(-k\varepsilon^2)$ $\varepsilon = R.T.ln(1 + \frac{1}{C_e})$ $E = \frac{1}{\sqrt{2B}}$	$Lnq_e = Lnq_m - B\varepsilon^2$	Dubinin-Radushkevcih	Sitthikhankaew et al. (2014); Azmi and Yunos (2014)
a_R: Redlich-Peterson isotherm constant $(1.mg^{-1})$ (b_R): Redlich-Peterson isotherm constant $(mL.mg^{-1})^a$ a: Power of Redlich-Peterson isotherm	$Ln(K_R \frac{C_e}{q_e} - 1) = gln(C_e) + ln(a_R)$	$q_e = \frac{q_m b_R C_e}{1 + b_R C_e^a}$	Redlich-Peterson	Azmi and Yunos (2014); Belala et al. (2011)
K_S: Sips isotherm constant $(mg/g)^{Bs}$ (ml.mg) βs: Sips isotherm constant without unit α_S: Sips isotherm constant without unit	$\beta_s ln(Ce) = -ln\frac{k_s}{q_e} + ln(\alpha_s)$	$q_e = \frac{q_m C_e^{\beta s}}{1 + \alpha_{\beta s} C_e^{\beta s}}$	Sips	Zouiten et al. (2016)

Assessment method of adsorption kinetics (non-equilibrium model)

To investigate the adsorption kinetics, the contact time was considered variable and other parameters as constant. The lead solution was prepared with the initial concentration of 10 mg.lit^{-1}. The pH of the solutions was adjusted to be 6. To each solution, 0.3 g of LCNFs was added, and then stirred at 25 °C in the incubator shaker (at 4000 rpm and 5 min) for the contact times of 15, 30, 60, 90 and 120 min. At the end, the used flasks were taken from the incubator shaker and then the centrifuge made the two-phase solution. The remaining heavy metal solution was measured by atomic absorption spectroscopy. The data from the kinetics were derived from the data of this section. Then, the matching of empirical data with the kinetic models was investigated and the curves for each model were drawn using its linear and nonlinear forms given in Table 2. The adsorption kinetic models can be divided into two groups: 1. Reaction-based models, and 2. Diffusion-based models (Klapiszewski et al., 2017). The models used in this study included reaction-based models of pseudo-zero-order, pseudo-first-order, pseudo-second-order and pseudo-third-order, and diffusion-based models of intra-particle diffusion and Elovich model. The pseudo-first-order kinetic equation is based on adsorbent capacity and is used when adsorption occurs through the diffusion process inside a boundary layer (physical adsorption) (Chowdhury et al., 2012[a]), while the pseudo-second-order kinetic equation shows that chemical adsorption is the dominant and controlling factor in the adsorption process (Chowdhury et al., 2012[b]). The Elovich kinetic model is based on adsorption capacity of adsorbent, and often is applicable to chemical absorption kinetics and systems with heterogeneous surfaces (Shirzad Siboni et al., 2012). Intraparticle diffusion is a diffusion-based kinetic model to describe the diffusion of solute molecules into the solid particles as well as competitive adsorption (Aharoni and Tompkins, 1970).

Table 2. Kinetic models and constant coefficients used in this research.

Parameters	Linear form	Equation	Equation	References
q_t : the amount of pollutant absorbed at time t q_0 : amount of pollutant absorbed at time zero	$qt=q_0 - K_0t$	-	Pseudo-zero order	Ayanda et al. (2013)
K_0: adsorption rate constant of pseudo-first-order (g.mg^{-1}.min^{-1}) q_e :amount of pollutant absorbed during equilibrium (mg.g^{-1}) K_1: adsorption rate constant of pseudo-first- order (min^{-1})	$\text{Log}(q_e-q_t)= \log q_e - \frac{K_1}{2.303}t$ $\text{Ln}(q_e-q_t)= \text{Ln}(qe-k_1.t)$	$\frac{dq_t}{d_t} = k_1(q_e - q_t)$	Pseudo-first order	Sekar et al. (2004)
K_2: adsorption rate constant of pseudo-second-order (g.mg^{-1}.min^{-1})	$\frac{t}{q_t} = \frac{1}{k_2 q_e} + \frac{1}{q_e}$ t	$\frac{dq}{dt} = k_2(q_e-q_t)^2$	Pseudo-second order	Teoh et al. (2013)
K_3: adsorption rate constant of pseudo-third-order (g.mg^{-2}.min^{-2})	$\frac{1}{{q_t}^2} = \frac{1}{{q_o}^2} - k_3t$	-	Pseudo-third order	Ho and McKay (2002)
α: initial adsorption level (mg.g.min^{-1}) β: desorption constant and activation energy in chemical reactions (g.mg^{-1})	$q_e= (\frac{1}{\beta})\ln(\alpha\beta)+(\frac{1}{\beta})\ln t$	$\frac{dq_t}{d_t} = \alpha \exp(-\beta q_t)$	Elovich	Nethaji et al. (2013); Uslu (2009)
C: thickness of adsorption boundary layer (mg.g^{-1})	$q_t= k_t^{0.5}+C$	-	Intra particle diffusion	Uslu (2009)

Assessment method of adsorption thermodynamics

The lead solution with the initial concentration of 10 mg/L was prepared to evaluate removal thermodynamics. The pH of the solutions was adjusted to be optimal. To each lead solution, 0.3 g of LCNFs was added, and then stirred at the temperatures of 15, 20, 25, 30 and 40 °C in the incubator shaker for 60 min. At last, the used flasks were taken from the incubator shaker and then the centrifuge made the two-phase solution at 4000 rpm for 5 min, and the solutions were prepared for measurements. The data from the thermodynamics were obtained from the data of this section. Then, the matching of empirical data with the thermodynamic models was investigated and the related curves were drawn. In order to determine the thermodynamic parameters, the values of 1/T versus Ln k_C were plotted. The resultant slope represents the value of ΔH◦ in Kj/mol and y-intercept expresses the parameter ΔS◦ in Kj/mol. The adsorption process was determined after plotting the curve and by calculating ΔH◦ and ΔS◦, spontaneity and exothermic or endothermic features. The three thermodynamic parameters that should be measured in the adsorption process include Gibbs free energy (ΔG), enthalpy (ΔH◦) and entropy (ΔS◦). The thermodynamics of lead adsorption by LCNFs and the parameters associated with each of these are as follows (Shi et al., 2013). The thermodynamic values were obtained using equations (4), (5) and (6), which are as follows:

$$G = -RTLn\ K_c\ \Delta \qquad \text{Equation (4)}$$

$$\Delta G = \Delta H - T\ \Delta S \qquad \text{Equation (5)}$$

$$Lnk_c = -\frac{\Delta H}{R}\frac{1}{T} + \frac{\Delta S}{R} \qquad \text{Equation (6)}$$

ΔG◦ represents the standard free energy variation in $J.mol^{-1}k^{-1}$. ΔH◦ and ΔS◦ respectively show enthalpy and entropy in $Kj.mol^{-1}$, R is universal gas constant in 314 $J.mol^{-1}.k^{-1}$, T is absolute temperature in K, and K_c expresses equilibrium constant and without unit (Rezaei, 2011 , Nuhoglu, and Malkoc, 2009; Maurya et al., 2014).

Results and Discussion

TEM images of LCNFs

In order to study the diameter of LCNFs, TEM analysis was applied. Figure 1 shows the TEM images of LCNFs; the diameter of the used material is less than 100 nm (in the range of nanometers) and with fiber and network structures. The mean diameter of LCNFs was 65±10 nm.

Figure 1. TEM images of LCNFs.

FT-IR analysis

The FT-IR analysis was used to determine the superficial groups of lignocellulose nanofiber. Figure 2 indicates the FT-IR spectra of lignocellulose nanofiber prior to the lead adsorption (red curve) and after lead adsorption (blue curve).

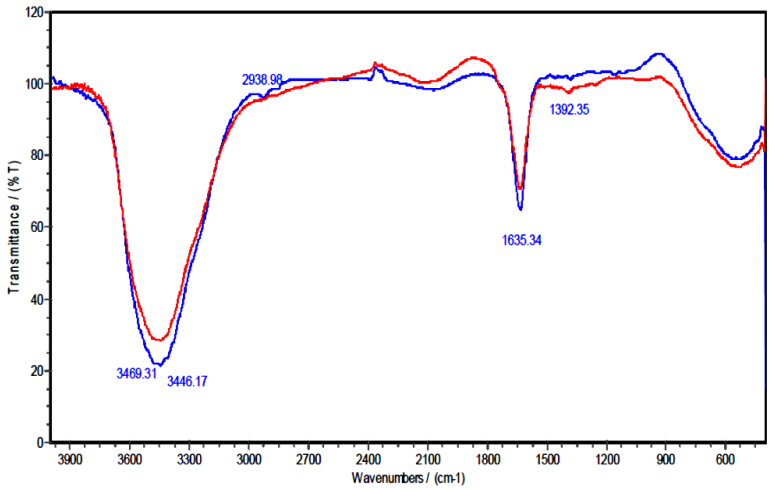

Figure 2. FT-IR spectroscopy of LCNFs before and after lead adsorption.

Tables 3 and 4 show the peaks of lignocellulose nanofiber before and after lead adsorption. As shown in Figure 3, the wide peak (the left side) in the region of 3000-3600 cm^{-1} (3469.31 cm^{1}) is related to the –OH (hydroxyl) or -NH functional groups in the FT-IR spectrum before absorbing lead by lignocellulose nanofiber. The peak in the region of 1635.34 cm^{-1} is related to the functional group of C=O. The next weak band in the region of 2098.17 cm^{-1} probably relates to the C≡C or C≡N functional groups. In the FTIR spectrum after absorbing lead by the lignocellulose nanofiber, the -OH group in 3469.31 cm^{-1} band was changed to 3461.6 cm^{-1} band after absorbing lead ions, and the C=O group in 1635.34 cm^{-1} band after absorbing lead ions was changed to 2861.84 cm^{-1}, which indicates the involvement of these functional groups in the adsorption process. The weak band in the region of 2925.48 cm^{-1} after adsorption is probably related to the SP^3 C-H stretch (C=C band in the region of 2098.17 cm^{-1} after being absorbed reacts with the lead and converts to C-C band in the region of 2925.48 cm^{-1}).

Table 3. FT-IR spectra of LCNFs before and after adsorption (cm^{-1}).

Before lead adsorption	3469.31	2098.17	1635.34	1392.35	543.83
After lead adsorption	3461.6	2925.48	2861.84	1635.34	1382.71

Table 4. FT-IR wavenumbers and functional groups of LCNFs.

Functional groups	Wavenumbers (cm^{-1})
OH- -NH	3469.31
C=O	1635.34
C≡C	2098.17
SP^3 C-H stretch	2925.45

Isotherm adsorption

With the fitting of six isotherm models including Langmuir, Freundlich, Sips, Temkin, Redlich-Peterson and Dubinin-Radushkevich on the adsorption equilibrium data, the results of each model test are presented in Tables 5 and 6 as well as Figures 3-8. The correlation coefficient (R^2) of two-parameter models of the Langmuir (0.9997), Freundlich (0.8064), Dubinin-

Radushkevich (0.6064), Temkin (0.8894) and correlation coefficient (R^2) of the three-parameter models of Redlich-Peterson (0.9338) and Sips (0.794) were obtained according to the graphs drawn in this study. Regarding the obtained correlation coefficients, the Langmuir isotherm among the two-parameter models, and the Redlich-Peterson isotherm among the three-parameter models had higher R^2. Finally, the Langmuir isotherm showed better fit with lead adsorption data due to higher correlation coefficient. Since the R^2 value of Langmuir model is close to 1, it is concluded that the data obtained from the experiment showed a slight deviation from the target model and there was an acceptable trend in the empirical data. The fitting of data with the Langmuir model showed that the lead adsorption on the LCNFs surface occurred homogeneously as monolayer. In addition, all reactive sites on the surface of LCNFs had the same absorption energy (Li et al., 2007).

In this research, the separation factor (RL=0.2266) of the Langmuir isotherm was between zero and one, which is the desirability of the adsorption process. The greater fitting between Langmuir and Redlich-Peterson models in this experiment is due to further closure of adsorbent cells over the adsorption process and the reduction of the influence of the side factors on lead adsorption (Igberase and Osifo, 2015). The E value obtained from the Dubinin-Radushkevich model was 8.57 kj / mol. The adsorption of lead ions by adsorbent LCNFs was accomplished by combining ion exchange and physical adsorption mechanisms. The positive values (B_T = +107.69) obtained from the Temkin model represent the exothermic adsorption process. Researchers have conducted similar studies to evaluate the adsorption isotherm in the lead removal efficiency. Mahajan and Sud (2013) examined the feasibility of using agricultural lignocellulose to remove nickel and lead for treatment of sewage. The equilibrium isotherm models of Freundlich, Langmuir and Temkin were investigated for lead adsorption. The Freundlich isotherm (multilayer) gave the best outcome, while the data were more fit with the Langmuir isotherm (monolayer). As a result, the findings contradicted the results of this section of the study (Mahajan and Sud, 2013). Zhang et al. (2017) used lignin to remove lead. The equilibrium isotherm models of Freundlich, Langmuir and Temkin were investigated for lead adsorption. The data were more consistent with the equilibrium isotherm (monolayer), so the results were in line with the findings of this section of the research.

Table 5. Data obtained from studying two-parameter isotherms in lead adsorption by LCNFs.

Isotherm models	Constant coefficients			
Langmuir	q_m (mg/g)	b (Lit/mg)	R_L	R^2
	3.034	-113.765	0.2266	0.9997
Freundlich	k_f (mg/g)	n		R^2
	3.0962	0.0296		0.8064
Dubinin-Radushkevcih	q_m (mg/gr)	E_{D-R} (Kj/mol)	K_{D-R} (mol^2/kj^2)	R^2
	2.88	8.57	-0.0068	0.6062
Temkin	A_T (L/gr)	B_T (j/mol)		R^2
	1	107.69		0.8894

Table 6. Data obtained from studying three-parameter isotherms in lead adsorption by LCNFs.

Isotherm models	Constant coefficients			
Redlich-Peterson	k_R $(L.mg^{-1})$	a_R $(L.mg^{-1})^g$	b_R (ml/mg)a	R^2
	1.108	0.3492	1.795	0.9338
Sips parameters	α_s $(L.mg^{-1})^B$	k_s $(mg.g^{-1})(L.mg^{-1})^B$	β_s $(ml/mg)^b$	R^2
	0.042	0.046	8.652	0.794

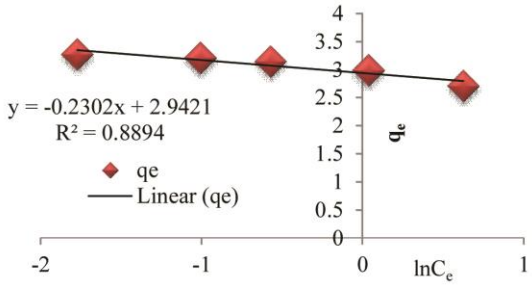

Figure 3. Temkin isotherm model for describing the lead adsorption process on LCNFs.

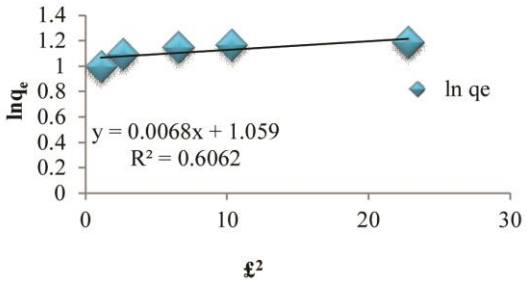

Figure 4. Dubinin-Radushkevich isotherm model for describing the lead adsorption process on lignocellulose nanofiber.

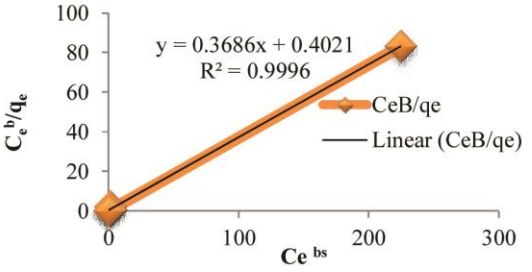

Figure 5. Sips isotherm model for describing the lead adsorption process on LCNFs.

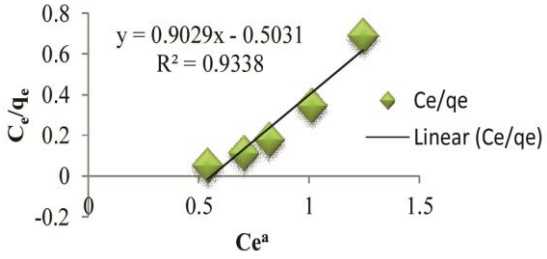

Figure 6. Redlich-Peterson isotherm model for describing the lead adsorption process on LCNFs.

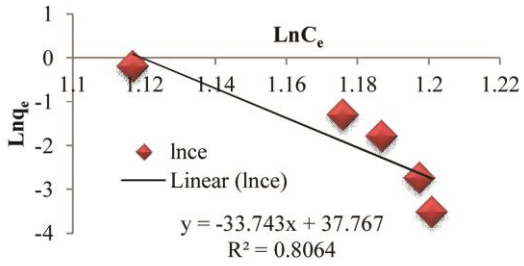

Figure 7. Freundlich isotherm model for describing the lead adsorption process on LCNFs.

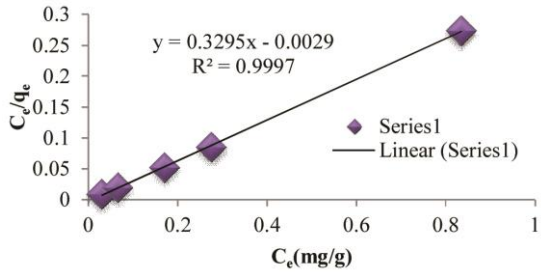

Figure 8. Langmuir isotherm model for describing the lead adsorption process on LCNFs.

Adsorption kinetics

Results of the lead adsorption kinetic models are presented in Table 7 and Figures 9-14 and the values of the constant coefficients of kinetic models for the adsorption process were investigated. The correlation coefficient (R^2) obtained for the reaction kinetic models of pseudo-zero-

order (0.6762), pseudo-first-order (0.9517), pseudo-second-order (1) and pseudo-third-order (0.6502) as well as for the diffusion kinetic models of intra-particle diffusion (0.7758) and Elovich (0.87) were obtained. Therefore, due to the higher correlation coefficients of pseudo-first- and second-order kinetics, it can be concluded that the empirical data obtained from lead adsorption experiments had higher fit with the pseudo-first- and second-order kinetics, but the data were better described by the pseudo-second-order model, so chemical adsorption was the dominant and controlling factor in the lead adsorption process, and the dominant mechanism controlling adsorption rate was not diffusion, but adsorption occurred on the adsorbent surface (Zawani et al., 2009).

As the obtained value of R^2 for this model and q_e and q_t values from the pseudo-second-order kinetic equation are less than q_t and q_e values from other kinetic models used in this research, they indicated the accuracy of the equilibrium test and confirmed the fit of lead removal by the adsorbent from the pseudo-second-order kinetic equation. The data obtained from the experiment showed conformance with the model and there was an acceptable trend in the empirical data. Researchers have conducted similar studies to investigate the effect of kinetics on lead removal. Ballav et al. (2015) used poly-aniline and lignocellulose composites to remove dye from aqueous solutions. Experiments were carried out in continuous and discontinuous (batch) systems. The adsorption kinetics of pseudo-first-order and pseudo-second-order were evaluated. The results showed that the data follow the pseudo-second-order kinetics, which is consistent with the results of this study. Anirudhan et al. (2016) applied nanocellulose/ nanobentonite composite to remove cobalt from the aqueous solutions. They studied adsorption kinetics and indicated that the data met the second-order kinetics that was consistent with the results of this study. Ren et al. (2016) removed lead using adsorbent Alginate/ Carboxymethyl/ Cellulose, and investigated adsorption kinetics of pseudo-first-order and pseudo-second-order. The results showed that the data followed the pseudo-second-order kinetics that was consistent with the results of this study.

Table 7. Data obtained from studying lead adsorption kinetic models by LCNFs.

Kinetic models	Constant coefficients		
Pseudo-zero order	K_0($g.mg^{-1}.min^{-1}$)	q_e($mg.g^{-1}$)	R^2
	0.0021	0.103	0.6762
Pseudo-first order	K_1 ($1.min^{-1}$)	q_e ($mg.g^{-1}$)	R^2
	0.0378	3.241	0.9517
Pseudo-second order	K_2 ($g.mg^{-1}.min^{-1}$)	q_e ($mg.g^{-1}$)	R^2
	0.2177	3.3602	1
Pseudo-third order	K_3 ($g.mg^{-2}.min^{-2}$)	q_e($mg.g^{-1}$)	R^2
	0.0001	3.1	0.6502
Intraparticle diffusion	C ($mg.g^{-1}$)	k_{dif} $(mg.g^{-1}.min^{-1})^{-1/2}$	R^2
	2.991	0.0333	0.7758
Elovich	α ($mg.g^{-1}min^{-1}$)	β ($g.mg^{-1}$)	R^2
	0.12	8.319	0.87

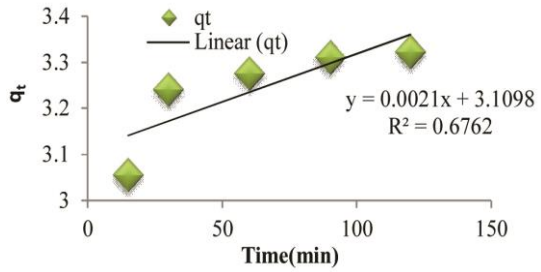

Figure 9. Pseudo-zero-order kinetic model of lead adsorption by LCNFs.

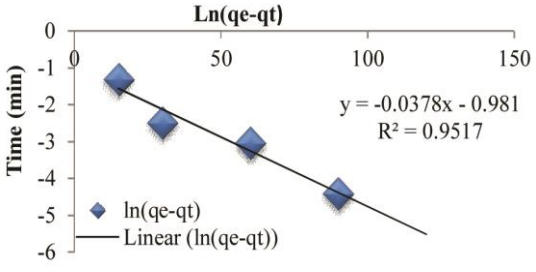

Figure 10. Pseudo-first-order kinetic model of lead adsorption by LCNFs.

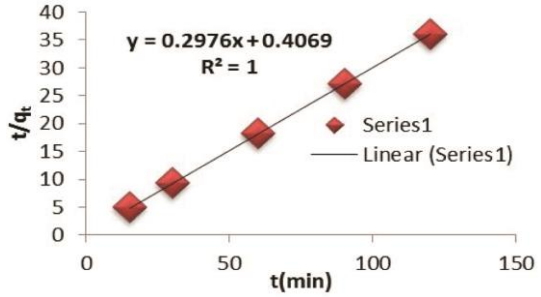

Figure 11. Pseudo-second-order kinetic model of lead adsorption by LCNFs.

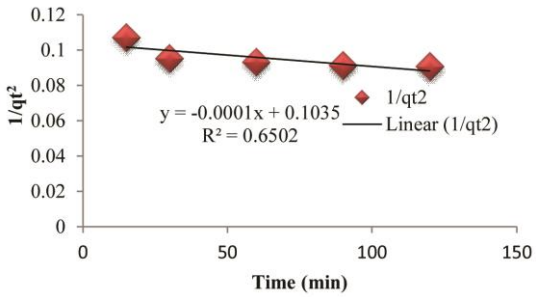

Figure 12. Pseudo-third-order kinetic model of lead adsorption by LCNFs.

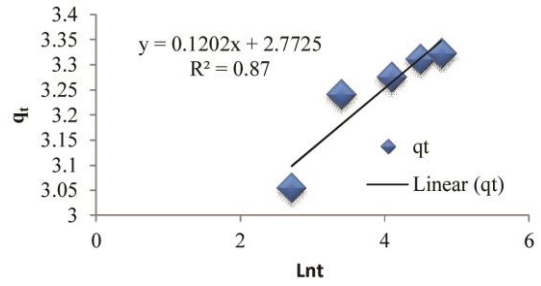

Figure 13. Elovich kinetic model of lead adsorption by LCNFs.

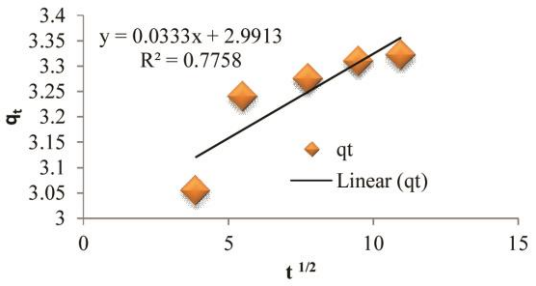

Figure 14. Intra-particle diffusion kinetic model of lead adsorption by LCNFs.

Thermodynamics

In the present study, according to the results of Figures 15, 16 and Table 8, the process of lead removal by LCNFs showed to be possible in terms of stoichiometry, indicating that the adsorption process is spontaneous. As the temperature rises, ΔG◦ (Gibbs free energy) is reduced; as a result, the spontaneous reaction of the process was increased. Additionally, the negative values of ΔH◦ (enthalpy) showed that the overall reaction process was exothermic, that is, the removal rate was increased by decreasing the ambient temperature. The high enthalpy changes indicate the sensitivity of the adsorption process to temperature (Duan et al., 2015). The positive values of ΔSº (entropy) also demonstrated that the amount of irregularity was increased at the solid-liquid interface during the adsorption process. In fact, the positive value of ΔS◦ represents the affinity of adsorbent to adsorbate in the solution and some structural changes in adsorbent and adsorbate. Researchers have done similar studies to investigate the thermodynamic effect on lead removal (Marciante and Murillo, 2017). Ge et al. (2016) used lignin for lead removal. The results of thermodynamics with respect to positive enthalpy values and high adsorption efficiency with increasing temperature

indicate the endothermic reaction, while in this study, the adsorption efficiency was decreased with increasing temperature, which indicates that the reaction was exothermic and therefore contradicted the results of this study. Klapiszewski et al. (2017) used Tion/Lignin as adsorbent to remove lead from aqueous solutions. The thermodynamic results of lead in terms of positive enthalpy values and high adsorption efficiency with increasing temperature demonstrate the endothermic reaction, which is also contrary to the results of this study.

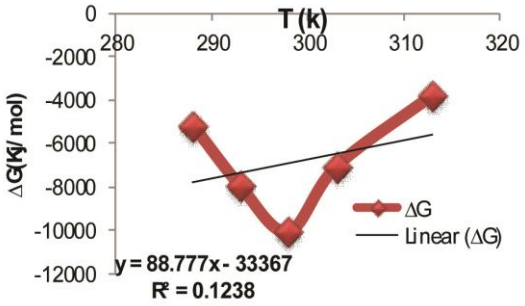

Figure 15. Gibbs free energy changes with temperature of lead adsorption by LCNFs.

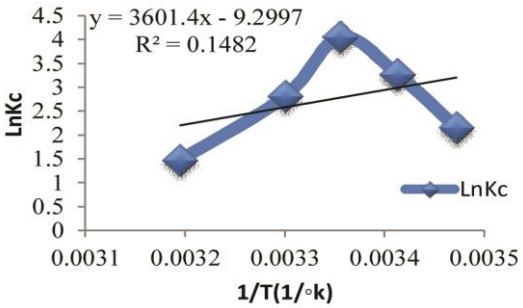

Figure 16. Changes in LnKc versus temperature of lead adsorption by LCNFs.

Table 8. Thermodynamic parameters in lead removal using LCNFs.

T(˚C)	T (K)	ΔG (kJ mol^{-1})	Δ*H*◦ (kJ mol^{-1})	Δ*S*◦ (J ×mol^{-1} × K^{-1})
15	288	-5169.4	-29942.04	+77.317706
20	293	-7973.67		
25	298	-10052.5		
30	303	-7092.28		
40	313	-3824.37		

Conclusion

The findings of the FT-IR spectrum revealed that the main structure of adsorbent LCNFs consists of carboxylic acid, and also the TEM images confirmed fiber and network nature of these adsorbents. Moreover, the isotherms, kinetics and thermodynamics of lead ion adsorption were investigated by adsorbent LCNFs. The results of studying the two-parameter isotherms (Langmuir, Freundlich, Redlich-Peterson and Temkin) and three-parameter isotherms (Redlich-Peterson and Sips) showed that the studied isotherms generally well predicted the system equilibrium. Correlation coefficients (R^2) from six adsorption isotherms showed that although the data were consistent with both Langmuir and Redlich-Peterson models, they were better described by the Langmuir model and indicated that lead adsorption on adsorbent was done as monolayer and homogeneous. The RL parameter from this model between zero and one suggests the desirability of the absorption system of this model. According to the results obtained from the review of reaction and diffusion kinetic models, the data were most consistent with pseudo-second-order kinetics (R^2=1); therefore, it can be concluded that the lead adsorption was of chemical type, more adsorption of cations on the adsorbent surface and penetration into pores has been achieved at a lower adsorption. In

conclusion, despite the changes in temperature, contact time and adsorbent dosage, because of the high flexibility of LCNFs, they are able to absorb high concentrations of lead metal from aqueous solutions, as well as due to high mechanical strength, wide contact surface and appropriate physical shape, they can be used to remove other heavy metals from water sources.

References

Afzal Kamboh, M., Wan Ibrahim, W.A., and Nodeh, H.R. 2016. The removal of organophosphorus pesticides from water using a new amino-substituted calixarene-based magnetic sporopollenin. New Journal of Chemistry, 4 (40), 3130-3148.

Aharoni, C., and Tompkins, F. 1970. Kinetics of adsorption and desorption and the Elovich equation. Adv. Catal. Relat. Subj. 21, 1-49.

Ahmad, A.L., Sumathi, S., and Hameed, B.H. 2005. Adsorption of residue oil from palm oil mill, effluent using powder and flake chitosan: equilibrium and kinetic studies. Water Res. 39 (12), 2483-2494.

Alam Khan, T., Mukhlif, A.A., Khan, E.A., and Sharma, D. 2016. Isotherm and kinetics modeling of Pb(II) and Cd(II) adsorptive uptake from aqueous solution by chemically modified green algal biomass, 2, 117.

Anirudhan, T.S., Deepa, J.R., and Christa, J. 2016. Nanocellulose/nanobentonite composite anchored with multi-carboxyl functional groups as an adsorbent for the effective removal of Cobalt(II) from nuclear industry wastewater samples, Journal of colloid and interface science, 467, 307-320.

Arvind, J., Bhattacharya, G., Keerthana, B., Soud, M., and Nachammai, S. 2017. Removal of nickel from synthetic waste water using gooseberry seeds as biosorbent, Journal of bioremediation and sustainable technologies for cleaner environment, 2, 103-118,

Ayanda, O.S., Fatoki, O.S., Adekola, F.A., and Ximba, B.J. 2013. Kinetics and equilibrium models for the sorption of tributyltin to nZnO, activated carbon and nZnO/activated carbon composite in artificial seawater, Marine pollution bulletin, 72 (1), 222-230.

Azmi, N.S., and Yunos, K.F.M. 2014. Wastewater Treatment of Palm Oil Mill Effluent (POME) by Ultrafiltration Membrane Separation Technique Coupled with Adsorption Treatment as Pretreatment. Agriculture and agricultural Science procedia. 2, 257-264.

Ballav, N., Debnath, S., Pillay, K., and Maity, A. 2015. Efficient removal of reactive black from aqueous solution using polyaniline coated ligno-cellulose composite as a potential adsorbent, Journal of molecular liquids, 209, 387-396.

Belala, Z., Jeguirim, M., Belhachemi, M., Addoun, F., and Trouvé, G. 2011. Biosorption of basic dye from aqueous solutions by date stones and palm-trees waste: kinetic, equilibrium and thermodynamic studies. Desalination. 271 (1-3), 80-87.

Betancur, M., Bonelli, P.R., Velásquez, J.A., and Cukierman, A.L. 2009. Potentiality of lignin from the Kraft pulping process for removal of trace nickel from wastewater: Effect of demineralization, J. Bioresours. Technol. 100 (3), 1130-1137.

Chowdhury, Z.Z., Zain, S.M., Khan, R.A., and Islam, M.S. 2012a. Preparation and characterizations of activated carbon from kenaf fiber for equilibrium adsorption studies of copper from wastewater. Korean J. Chem. Eng. 29 (9), 1187-1195.

Chowdhury, Z.Z., Zain, S.M., Khan, R.A., Rafique, R.F., and Khalid, K. 2012b. Batch and fixed bed adsorption studies of lead (II) cations from aqueous solutions onto granular activated carbon derived from Mangostana garcinia shell, BioResources. 7 (3), 2895-2915.

Duan, S., Tang, R., Xue, Z., Zhang, X., Zhao, Y., Zhang, W., Zhang, J., Wang, B., Zeng, S., and Sun, D. 2015. Effective removal of Pb (II) using magnetic Co 0.6 Fe 2.4 O 4 micro-particles as the adsorbent: synthesis and study on the kinetic and thermodynamic behaviors for its adsorption. Colloids Surf. A: Physicochem. Eng. Aspects. 469, 211-223.

Elagiwu, S.E., Usman, L.A., Awolola, G.V., Adebayo, G.B., and Ajayi, R.M.K. 2009. Adsorption of pb(ll) from aqueous solution by activated carbon prepared from Cow Dung, J. Adv. Natur. Sci. 3 (3), 442-446.

Ge, Y., Wu, S., Qin, L., and Zhili, L. 2016. Conversion of organosolv lignin into an efficient mercury ion adsorbent by a microwave-assisted method, Journal of the taiwan institute of chemical engineers, 63, 500-505.

Ho, Y.S., and McKay, G. 2002. Application of kinetic models to the sorption of copper (II) on to peat, Adsorption science and technology, 20, 797-815.

Huang, G., Wanga, D., Mab, S., Chen, J., Jiang, L., and Wang, P. 2015. A new, low-cost adsorbent: Preparation, characterization, and adsorption behavior of Pb (II) and Cu (II), Journal of colloid and interface science, 445, 294-302.

Igberase, E., and Osifo, P.O. 2015. Equilibrium, kinetic, thermodynamic and desorption studies of cadmium and lead by polyaniline grafted cross-linked chitosan beads from aqueous solution, J. Ind. Eng. Chem. 26, 340-347.

Inagaki, S., Caretta, T., Alfaya, R.V., and Alfaya, A. 2013. Mexerica mandarin (Citrus nobilis) peel as a new biosorbent to remove Cu(II), Cd(II), and Pb(II) from industrial effluent. Desalin, Water Treat. 51 (28-30), 5537-5546.

Kardam, A., Rohit Raj, K., Srivastava, S., and Srivastava, M.M. 2014. Nanocellulose fibers for biosorption of Cadmium nichkel, and Lead ions from aqueous solution, Clean technology and environmental policy, 16 (2), 385-393.

Kiapiszewski, K., Siwinska-Stefanska, K., and Kolodynska, D. 2017. Preparation and characterization of novel TiO_2/lignin and TiO_2-SiO_2/lignin hybrids and their use as functional biosorbents for Pb(II), Chemical Engineering Journal, 314, 169-181.

Kini Srinivas, M., Saidutta, M.B., Murty, V.R.C., and Kadoli Sandip, V. 2013. Adsorption of basic dye from aqueous solution using HCl treated sawdust (*Lagerstroemia microcarpa*): kinetic, modeling of equilibrium, thermodynamic, International Research Journal of Environment Sciences, 2 (8), 6-16.

Klapiszewski, L., Bartzak, P., and Jesionowski, T. 2017. Removal of lead (II) Removal of leadions by an adsorption process with the use of an advanced SiO_2/lignin biosorbent, Polish Journal of Chemical Technology, 19 (1), 67-74.

Kolodynska, D., Halas, P., Franus, M., and Hubicki, Z. 2017. Zeolite properties improvement by chitosan modification-Sorption studies, Journal of industrial and engineering chemistry, 52, 187-196.

Largitte, L., Burdey, T., Tant, T., Dumensnill, P., and Lodewyckx, P. 2016. Comparison of the adsorption of lead by activated carbons from three lignocellulosic precursors, Journal of microporous and mesoporous materials, 219, 265-275.

Li, Q., Zhai, J., Zhang, W., Wang, M., and Zhou, J. 2007. Kinetic studies of adsorption of pb(ll), Cr(ll) and Cu(ll) from aqueous Solution by sawdust and modified peanut husk, Journal of hazardous materials, 14 (4), 163-167.

Lopicic, Z.R., Stojanovic, M.D, Marovic, S.B., Milojikovic, J.V., Mihajilovic, M.L., Radoicic, T.S., and Kijevcanin, M.L. 2016. Effects of different mechanical treatments on structural changes of lignocellulosic waste biomass and subsequent Cu(II) removal kinetics, Arabian journal of chemistry, 5, 120-129.

Mahajan, G., and Sud, D. 2013. Application of Ligno-Cellulosic Waste Materisal for heavy metal removal from aqueous metal ions removal ions removal from aqueous solution. Journal of environmental chemical engineering, 1 (4), 1020-1027.

Marciante1, M., and Murillo, M.S. 2017. Thermodynamic and Kinetic Properties of Shocks in Two-Dimensional Yukawa Systems, Journal of biological chemistry, 292 (3), 955-966.

Maurya, R., Ghosh, T., Paliwal, C., Shrivastav, A., Chokshi, K., Pancha, I., Ghos, A., and Mishra, S. 2014. Biosorption of Methylene Blue by De-Oiled Algal Biomass: Equilibrium, Kinetics and Artificial Neural Network Modelling. PLoS ONE 9(10): e109545. doi:10.1371/ journal.pone.0109545.

Melichova, Z., and Romada, L. 2013. Adsorption of pb^{2+} and Cu^{2+} Ions from Aqqueous Solution On Natural Bentonite, Poly. Environ. Stud. 22 (2), 457-464.

Mohammed, R.R. 2013. Decolorisation of biologically treated palm oil mill effluent (POME) using adsorption technique, IRJES. 2 (10), 1-11.

Nagpal,UMK. and Rezaei, H. 2010. Equilibrium sorption studies for Cu^{2+} and Pb^{2+} metal ions on three different biomasses, Current World Environment 5 (2), 243.

Nasiruddin Khan, M., Bhutto, S., Wasim, A.A., and Khushid, S. 2016. Removal studies of Lead activated carbon derived from Lignocellulose Mangifera indicaseed shell, Journal of toxicological and environmental chemistry, 57 (24), 11211-11220.

Nethaji, S., Sivasamy, A., and Mandel, A. 2013. Adsorption isotherms, kinetics and mechanism for the adsorption of cationic and anionic dyes onto carbonaceous particles prepared from *Juglans regia* shell biomass, International journal of environmental science and technology, 10 (2), 231-242.

Niknahad Gharmakher, H., Esfandyari, A., and Rezaei, H., 2018. Phytoremediation of cadmium and nickel using Vetiveria zizanioides, Environmental Resources Research 6 (1), 41-50.

Nuhoglu, Y., and Malkoc, E. 2009. Thermodynamic and kinetic studies for environmentally friendly Ni (II) biosorption using waste pomace of olive oil factory. Bioresour Technol. 100, 2375-2380.

Ozcan, A.S., Ozcan, A., Tunali, S., Akar, T., Kiran, I., and Gedikbey, T. 2007. Adsoorption potential of Lead (ll) Ions from Aqueous Solution onto Capisicum anuum Seeds, J. Sep. Sci. Tech. 42, 137-151.

Parhizgar, F., Alishahi, A., Varasteh, H., and Rezaee, H. 2017. Removing sodium dodecyl benzene sulfonate (SDBS) from aqueous solutions using chitosan, Journal of Polymers and the Environment 25 (3), 836-843.

Reddy, D.H.K., and Lee, S.M. 2013. Application of magnetic Chitosan Composites for the removal of Toxic metal and dyes from aqueous solution. Journal of advances in colloid and interface science, 201-202, 68-93.

Ren, H., Gao, Z., Wu, D., Jiang, J., Sun, Y., and Luo, C. 2016. Efficient Pb(II) removal using sodium alginate–carboxymethyl cellulose gel beads: Preparation, characterization, and adsorption mechanism, Carbohydrate polymers, 137, 402-409.

Rezaei, H., Kulkarni, SD. and Saptarshi, PG. 2011. Study of Physical Chemistry on Biosorption of Nickel by using Chlorella pyrenoidosa, Oriental Journal of Chemistry 27 (2), 595-602.

Salamat, S., Hadavifar,M., and Rezaei, H. 2019. Preparation of nanochitosan-STP from shrimp shell and its application in removing of malachite green from aqueous solutions Journal of Environmental Chemical Engineering 7 (5), 103328.

Saman, N., Joharib, K., Songa, S.T., Konga, H., Cheua, S.C., and Mat, H. 2017. High removal efficacy of Hg(II) and MeHg(II) ions from aqueous solution by organoalkoxysilane-grafted lignocellulosic waste biomass, Journal of chemosphere, 171, 19-30.

Sekar, M., Sakthi, V., and Rengaraj, S. 2004. Kinetics, equilibrium adsorption study of lead (ll) onto activated carbon prepared from coconut Shell, Journal of colloid and interface science, 79, 307-313.

Shahmohaammadi Kalagh, S., Babazadeh, H., Nazemi, A.H., and Manshuri, M. 2011. Isotherm and kinetic studies on adsorption of Pb, Zn and Cu by kaolinite caspian, J. Env. Sci. 9 (2), 243-255.

Shahat, A., Awual, M.R., Abdul khaleque, M., and Alam, Z. 2015. Large-pore diameter nano-adsorbent and its application for rapid Lead (ll) detection and removal From aqueous medi, J. Chem. Eng. http://dx.doi.Org/10.1016/j/Cej.2015.03.073.

Shi, Y., Kong, X., Zhang, C., Chen, Y., and Hua, Y. 2013. Adsorption of soy isoflavones by activated carbon: Kinetics, thermodynamics and influence of soy oligosaccharides. Chem. Eng. J. 215-216, 113-121.

Shirzad Siboni, M., Samadi, M.T., Yang, J.K., and Lee, S.M. 2012. Photocatalytic removal of Cr (VI) and Ni (II) by UV/TiO2: kinetic study, Desalination and water treatment, 40 (1-3), 77-83.

Sitthikhankaew, R., Chadwick, D., Assabumrungrat, S., and Laosiripojana, N. 2014. Effects of humidity, O_2 and CO_2 on H_2S adsorption onto upgraded and KOH impregnated activated carbons, Fuel process technology, 124, 249-257.

Teoh, Y.P., Ali Khan, M., and Choong, T.S.Y. 2013. Kinetic and isotherm studies for lead adsorption from aqueous phase on carbon coated monolith, Chemical engineering journal, 217, 248-255.

Uslu, H. 2009. Adsorption equilibria of formic acid by weakly basic adsorbent Amberlite IRA-67: Equilibrium, kinetics, thermodynamic, Chem. Eng. 155 (1-2), 320-325.

Wang, L., Zhang, J., Zhao, R., Li, Y., Li, C., and Zhang, C. 2010. Adsorption of Pb(II) on activated carbon prepared from Polygonum orientale Linn.: kinetics isotherms, pH, and ionic strength studies, Bioresource Technology, 101, 5808-5814.

Yang, R., Aubercht, K.B., Ma, H., Wang, R., Grubbs, R.B., Hsiao, B.S., and Chu, B. 2014. Thiol-modiefiesd cellulose nanofibrous composite membranes for chromium (VI) and lead (ll) Adsorption, Journal of polymer, 55 (5), 1167-1176.

Yu, B., Zhang,Y., Shukla, A., and Shukla, S. 2001. Dorris Solution by Sawdust adsorption – removed of Lead and Comparison of its adsorption with Copper, Journal of hazardous materials, B. 84, 83-94.

Zawani, Z., Luqman, C.A., and Thomas, S.Y.C. 2009. Equilibrium, kinetics and thermodynamic studies: adsorption of remazol black 5 on the palm kernel shell activated carbon (PKSAC). Eur. J. Sci. Res. 3 (1), 763-771.

Zhang, X., Jin, C., Jiang, Y., Liu, G., and Wu, G. 2017. A novel gallic acid-grafted-lignin biosorbent for the selective eemoval of lead ions from aqueous solutions, Bioresources, 12 (3), 210-218.

Zouiten, A., Beltifa, A., Van Loco, J., Ben Mansour, H., and Reyns, T. 2016. Ecotoxicological potential of antibiotic pollution–industrial wastewater: bioavailability, biomarkers, and occurrence in Mytilus galloprovincialis, Environmental science and pollution research. doi:10.1007/s11356-016-6713-2.